17 (2023) 100297

Contents lists available at ScienceDirect

International Journal of Thermofluids

journal homepage: www.sciencedirect.com/journal/international-journal-of-thermofluids

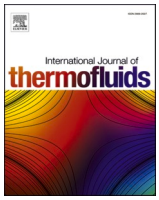

An investigation to identify the performance of cascade refrigeration system by adopting high-temperature circuit refrigerant R1233zd(E) over R161

Vivek K. Patel [a], Bansi D. Raja [b], Parth Prajapati [a], Laxmikant Parmar [a], Hussam Jouhara [c,d,*]

[a] Department of Mechanical Engineering, Pandit Deendayal Energy University, Gandhinagar, Gujarat, India
[b] Department of Mechanical Engineering, Indus University, Ahmedabad, Gujarat, India
[c] Heat Pipe and Thermal Management Research Group, College of Engineering, Design and Physical Sciences, Brunel University London, UB8 3PH, United Kingdom
[d] Vytautas Magnus University, Studentu Str. 11, LT-53362 Akademija, Kaunas Distr., Lithuania

ARTICLE INFO

Keywords:
Cascade refrigeration
Exergy efficiency
Total cost
Optimization
Thermo-economic analysis

ABSTRACT

In this work, the refrigerant R1233zd(E) (A1 ASHRAE safety code) is investigated for the possible substitution of refrigerant R161 (A2 ASHRAE safety code) in a cascade refrigeration system. The high-temperature circuit refrigerant R1233zd(E) is evaluated with the low-temperature circuit refrigerants R41 and R170 for thermo-economic consideration. A comparative analysis of the refrigerant combination R41-R1233zd(E) and R170-R1233zd(E) presents exergy efficiency and total plant cost as evaluation criteria. Pareto solutions are obtained for the thermo-economic objectives for each pair of refrigerants. A decision-making method is adopted to identify the best result from the Pareto solutions obtained. The effects of operating variables such as evaporator temperature, condenser temperature, LTC condensing temperature, and temperature difference of cascade condenser are evaluated. The sensitivity of the operating variables on thermo-economic objectives is also evaluated. The comparative results reveal that for the same total cost rate of the system (68,615 $/year), the exergy efficiencies of the CRS are 63.08% (R170-R161), 64.04% (R41-R161), 64.93% (R170-R1233zd(E)), and 65.81% (R41-R1233zd(E)). Also, the R1233zd(E) based CRS operates with a lower total cost rate than the R161-based system.

1. Introduction

Low-temperature requirements are essential in various industries such as chemical, food, petroleum, medical sectors, etc. [1–3]. Vapor compression refrigeration (VCR) is generally used in various industrial applications which require low temperatures. However, with a reduction in the low temperature required, a single-stage VCR system is not an economical option due to the high compression work. Compressor maintenance costs also increase due to increased wear and tear. In such applications, a multi-stage VCR system or cascade refrigeration system (CRS) is a good option for obtaining the desired cooling effect with considerable economy [4,5].

A cascade refrigeration system is a multi-stage refrigeration system where two or more individual VCR systems are coupled at the condenser-evaporator stage. In a two-stage cascade, the condenser of a low-temperature circuit (LTC) is coupled with the evaporator of a high-temperature circuit (HTC). The refrigerant of the LTC takes heat from the cooling space through its evaporator and gives it to the HTC refrigerant through the cascade condenser, and the HTC refrigerant transfers that heat to the atmosphere through the HTC condenser [6,7]. Refrigerants belonging to Chlorofluorocarbon (CFC), Hydrofluorocarbon (HFC), and Hydrocarbon (HC) categories are used in the LTC and HTC of CRS. HFCs and CFCs are known to be greenhouse gasses with considerable global warming potential (GWP), while HCs are flammable and toxic [8,9]. The refrigerants belonging to HFO (Hydrofluoro-olefin) and HCFO (Hydrochlorofluoro-olefin) categories have relatively lower GWP than CFC and HFC refrigerants. Hence, researchers have investigated the thermo-economic performance of the CRS with HFO and HCFO refrigerants [10].

Aktemure et al. [11] conducted a comparative analysis based on CRS's energy and exergy efficiency with low GWP halogen-based refrigerants R1243zf, R423A, R601, R601A, R1233zd (E), and R170 in the HTC and R41 in the LTC. The authors reported that R170 is the best and R423 is the worst refrigerant when paired with R41. Sun et al. [12] performed energy and exergy analysis on groups of refrigerants for CRS

* Corresponding author.
E-mail address: Hussam.Jouhara@brunel.ac.uk (H. Jouhara).

https://doi.org/10.1016/j.ijft.2023.100297
Received 1 December 2022; Received in revised form 17 January 2023; Accepted 29 January 2023
Available online 31 January 2023

Nomenclature

A	Area (m^2)
C	Capital cost ($)
$\dot{C}$	Cost rate ($.year^{-1})
ED	Exergy destruction (kJ.s^{-1})
Ex	Exergy (kJ.s^{-1})
h	Enthalpy (kJ.kg^{-1})
i	interest rate (%)
$\dot{m}$	Mass flow rate (kg.s^{-1})
n	plant life cycle
N	Annual operational hours (hr)
s	entropy (kJ.kg^{-1}.K^{-1})
T	temperature
W	Work input (kW)

Greek symbols

α	Cost ($)
η	Efficiency
μ	Emission factor
φ	Maintenance factor

Subscripts

cas	cascade condenser
cond	Condenser
elec	Electrical
eva	Evaporator
HTC_{comp}	High temperature circuit compressor
HTC_{exp}	High temperature circuit expansion valve
LTC_{comp}	Low temperature circuit compressor
LTC_{exp}	Low temperature circuit expansion valve
s	Isentropic

and concluded that R41-R161 and R170-R161 are the best combinations with evaporator temperatures less than −60°C and more than −60°C, respectively. Ustaoglu et al. [13] studied CRS for thermodynamic and exergy considerations by performing optimization and parametric analysis. The authors considered R744 as a LTC refrigerant and R134a as a HTC refrigerant in their analysis and adopted Taguchi and ANOVA methods for the optimization. Sun et al. [14] studied different pairs of refrigerants for a three-stage CRS. The authors show the effect of evaporation temperature on the coefficient of performance (COP), pressure ratio, compression power, exergy efficiency, and exergy destruction of each component. Based on the simulation, the author recommended R14 for the LTC, R41, and R161 for the HTC. Roy et al. [15] performed an energy and economic optimization of a two-stage CRS with different pairs of refrigerants. Based on the optimization results, the authors reported that R41 and R170 refrigerants yield better thermo-economic performance with R161 HTC refrigerant. Yilmaz et al. [16] compared the thermodynamic performance of a cascade system for heating and cooling applications using CO_2 as the working fluid in LTC and HFE 7000, R134a, R152a, R32, R1234yf, and R365mfc refrigerants in HTC.

Singh et al. [17] performed an energy and economic analysis of CRS with a flash tank in the HTC and an intercooler in the LTC using a pair of natural refrigerants. The authors reported that R717-R290 is the best natural refrigerant combination for CRS. Patel et al. [18] compared a two-stage CRS operated with natural refrigerants based on thermo-economic criteria. The authors also identified the effect of each component on the economic performance of the system. Keshtkar [19] performed exergetic and economic optimization of CRS with R134a and R744 as HTC and LTC refrigerants. The authors studied the effect of evaporator temperature, condenser temperature, and degree of superheating on the CRS performance. Ust and Karakurt [20] presented an analysis and optimization of CRS by taking COP and exergetic performance coefficient (EPC) into consideration. The authors reported that R23-R717 provides a better performance than R23–290, R23–404A, and R23–507A. Mosaffa et al. [21] performed the exergetic and economic optimization of a two-stage CRS equipped with a flash tank and flash intercooler. The authors considered natural refrigerants in their study. Qin et al. [22] presented a comparative analysis of a three-stage CRS for ultra-low temperature in the range of −100 °C. The authors reported that the R1234yf-R23-R14 refrigerant combination provides maximum COP and exergetic efficiency. In the study by Yilmaz et al. [23], HFE7000 was investigated thermodynamically in the cascade cooling system. The effect of different parameters on the system's COP, energy efficiency and exergy efficiency was studied.

It can be observed from the literature survey that researchers have explored various refrigerants belonging to the HFC, HC, CFC, HCFO, and HFO categories for the HTC of the cascade refrigeration system. However, most refrigerants explored belong to A2 and A3 ASHRAE safety codes [24]. Further, only a few systematic comparisons of refrigerants are observed in the literature. Considering this fact, in the present work, an effort has been made to investigate a refrigerant belonging to the A1 ASHRAE safety code for the HTC of a cascade refrigeration system. The purpose of this paper is to present a comparative analysis of the A1 ASHRAE safety code HTC refrigerant R1233zd(E) with R41 and R170 LTC refrigerants. A detailed comparative analysis of the considered A1 code HTC refrigerant is presented in this paper, which can be taken as a basis for the possible substitution of the currently used A2 or A3 code HTC refrigerants.

The main contributions of the work are: a) to investigate the A1 ASHRAE code HTC refrigerant R1233zd(E) with R41 and R170 LTC refrigerants based on thermo-economic considerations; b) a detailed analysis of R41-R1233zd(E) and R170-R1233zd(E) based CRS and their comparison with R41-R161 and R170-R161 based CRS; c) to identify the effect of operating variables on the component cost, total cost, and exergy efficiency of the R41-R1233zd(E) and R170-R1233zd(E) based CRS; d) to analyze the behavior of each operating variable for the sensitivity of thermo-economic objectives of CRS. A thermal model of CRS is developed for the thermo-economic analysis and optimization. The CRS's total plant cost rate and exergy efficiency are analyzed by adapting a multi-objective heat transfer search algorithm.

The above contributions are demonstrated by considering a case study of a two-stage CRS. The organization of the rest of the paper includes a system description and formulation of energy, exergy, and economic modeling (Section 2); the framework of system optimization with operating variables and objective function (Section 3); a brief description of the heat transfer search algorithm and its multi-objective variant (Section 4); a case study, result-discussion and comparative analysis (Section 5); and finally conclusions of the work described in Section 6.

2. System description and energy, exergy & economic modeling of CRS

This section briefly describes a two-stage CRS and its energy, exergy, and economic modeling. Fig. 1 shows a schematic arrangement of a two-stage CRS system along with its thermodynamic presentation in the form of a pressure-enthalpy chart. As mentioned previously, two single-stage VCR systems (i.e. LTC and HTC) are coupled together with the help of a cascade condenser. The LTC evaporator absorbs heat from the cooling space and rejects heat to the HTC via a cascade condenser, and the HTC rejects heat to the atmosphere at its condenser. In the present investigation, R41 and R170 refrigerants are considered for the LTC while

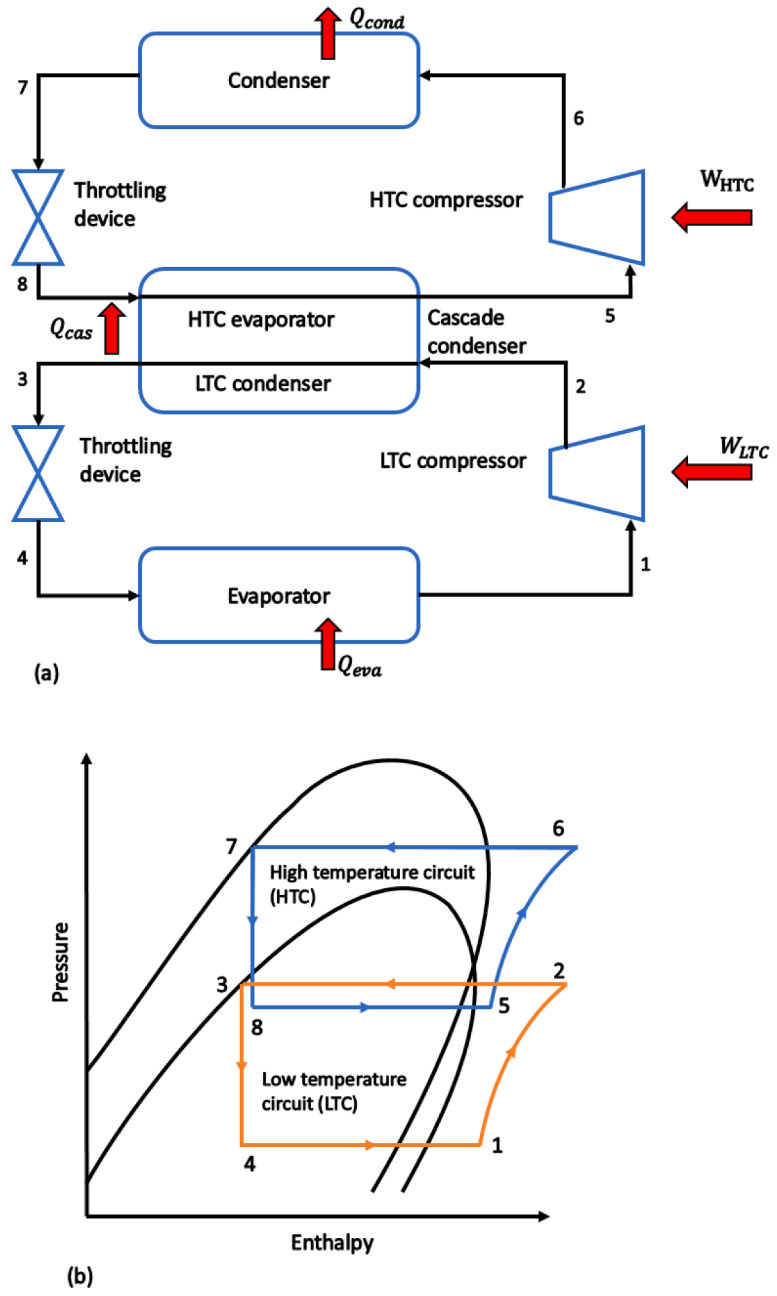

Fig. 1. Cascade refrigeration system (a) schematic diagram (b) P-h diagram.

R1233zd(E) is used as the refrigerant for the HTC. The different state points (i.e. points 1, 2,….,8) on the schematic and thermodynamic chart indicate the conditions of refrigerants at the inlet/outlet of different components of the LTC and HTC.

2.1. Energy and exergy modeling

The following assumptions are considered while developing energy and exergy modeling of the CRS.

- Ø Negligible change in the potential and kinetic energies of the refrigerants and hence energy and exergy can be calculated from enthalpy and entropy.
- Ø Superheat cycles with no subcooling in LTC and HTC.
- Ø All components of LTC and HTC run under steady-state conditions.

The mass flow rate of refrigerant in the LTC of the CRS is calculated by [21,25]

$$\dot{m}_{LTC} = \frac{Q_{eva}}{h_1 - h_4} \tag{1}$$

where Q_{eva} is the cooling load of the system, h_1 and h_4 are the enthalpies of the refrigerant at state points 1 and 4 of the LTC.

Likewise, the mass flow rate of the refrigerant in the HTC is calculated by

$$\dot{m}_{HTC} = \frac{Q_{cas}}{h_5 - h_8} \tag{2}$$

where Q_{cas} is the rate of heat transfer in the cascade condenser and it can be calculated as

$$Q_{cas} = \dot{m}_{LTC}(h_2 - h_3) = \dot{m}_{HTC}(h_5 - h_8) \tag{3}$$

The condenser heat transfer in the HTC is calculated as:

$$Q_{cond} = \dot{m}_{LTC}(h_6 - h_7) \tag{4}$$

The work required to run LTC and HTC compressors is obtained by

$$W_{LTC} = \frac{m_{LTC}(h_2 - h_1)}{\eta_s \eta_m \eta_{elec}} \tag{5}$$

$$W_{HTC} = \frac{m_{HTC}(h_6 - h_5)}{\eta_s \eta_m \eta_{elec}} \tag{6}$$

where η_s is the isentropic efficiency, η_m is the mechanical efficiency, and η_{elec} is the electrical efficiency of the compressor

Total compressor power required to run the CRS can be calculated by

$$W_{total} = W_{LTC} + W_{HTC} \tag{7}$$

So, the COP of the CRS can be calculated as

$$COP = \frac{Q_{eva}}{W_{total}} \tag{8}$$

The exergy of the refrigerants in HTC and LTC for every state (i.e. 1, 2, ….,8) can be calculated by

$$Ex_j = \dot{m}\left[\left(h_j - h_0\right) - T_0\left(s_j - s_0\right)\right] \tag{9}$$

where subscript j represents the state of refrigerant corresponding to Fig. 1. h_0 & s_0 represent enthalpy and entropy of the refrigerant at atmospheric conditions, and T_0 is the atmospheric temperature.

To obtain the total exergy destruction of the system (ED_{total}), the value of exergy destruction (ED) for each component can be calculated as below:

$$ED_{eva} = Ex_4 - Ex_1 + Q_{eva} * \left(1 - \left(\frac{T_0}{T_{eva}}\right)\right) \tag{10}$$

$$ED_{LTC_{comp}} = Ex_1 - Ex_2 + W_{LTC} \tag{11}$$

$$ED_{cas} = Ex_2 + Ex_8 - Ex_3 - Ex_5 \tag{12}$$

$$ED_{LTC_{exp}} = Ex_3 - Ex_4 \tag{13}$$

$$ED_{HTC_{comp}} = Ex_5 - Ex_6 + W_{HTC} \tag{14}$$

$$ED_{HTC_{exp}} = Ex_7 - Ex_8 \tag{15}$$

$$ED_{cond} = Ex_6 - Ex_7 - Q_{cond} * \left(1 - \left(\frac{T_0}{T_{cond}}\right)\right) \tag{16}$$

$$ED_{total} = ED_{eva} + ED_{LTC_{comp}} + ED_{cas} + ED_{LTC_{exp}} + ED_{HTC_{comp}} + ED_{HTC_{exp}} + ED_{cond} \tag{17}$$

where the subscripts to ED indicate the exergy destruction of corresponding components.

Finally, the exergy efficiency of the CRS can be calculated as

$$\eta_{ex} = \frac{W_{total} - ED_{total}}{W_{total}} \tag{18}$$

2.2. Economic modeling

The total cost rate of the CRS consists of the capital and maintenance cost rate ($\dot{C}_k$), the operating cost rate ($\dot{C}_{OP}$), and the environmental cost rate ($\dot{C}_{env}$) associated with the different components of the system. The total plant cost rate of the CRS is given as,

$$C_{total} = \sum_K \dot{C}_k + \dot{C}_{OP} \tag{19}$$

The capital and maintenance cost rate of the CRS is calculated as below [21,26],

$$\dot{C}_k = C_C * \varphi * CRF \tag{20}$$

where C_c is the capital cost of each component, φ is the maintenance factor and CRF is the capital recovery factor.

The capital cost of each component (i.e. HTC & LTC compressor and expansion valve, evaporator, cascade condenser, and condenser) are listed below [21,26]

$$C_{HTC_{comp}} = 9624.2 * W_{HTC}^{0.46} \tag{21}$$

$$C_{LTCC_{comp}} = 10,167.2 * W_{HTC}^{0.46} \tag{22}$$

$$C_{HTC_{exp}} = 114.5 * \dot{m}_{HTC} \tag{23}$$

$$C_{HTC_{exp}} = 114.5 * \dot{m}_{LTC} \tag{24}$$

$$C_{eva} = 1397 * A_{eva}^{0.89} \tag{25}$$

$$C_{cond} = 1397 * A_{cond}^{0.89} \tag{26}$$

$$C_{cas} = 383.5 * A_{cas}^{0.65} \tag{27}$$

CRF depends on the plant life (n) and interest rate (i) and is calculated as below,

$$CRF = \frac{i(i+1)^n}{(1+i)^n - 1} \tag{28}$$

The operational cost of the system depends on the power consumption required to run compressors and it is given by

$$\dot{C}_{OP} = N * W_{total} * \alpha_{elec} \tag{29}$$

where N and α_{elec} are the annual operational hours and electrical power cost respectively.

The environmental cost rate contains penalty costs due to CO_2 emissions from the electricity generation plant which is required to run compressors, and it can be estimated as [27]

$$\dot{C}_{env} = m_{CO_2e} * C_{CO_2} \tag{30}$$

where C_{CO_2} is the cost of CO_2 avoided, m_{CO_2e} is the annual CO_2 emission from the plant which can be calculated as

$$m_{CO_2e} = \mu_{CO_2e} * E_{annual} \tag{31}$$

where μ_{CO_2e} and E_{annual} are the emission factor and annual electricity consumption, respectively.

The energy, exergy, and economic modeling described above formulate the thermo-economic objective function described in the next section.

3. Objective function formulation, operating variables, and framework of system optimization

The present work investigates a comparative analysis of R41-R1233zd(E) and R170-R1233zd(E) based CRS through thermo-economic optimization. Maximizing exergy efficiency and minimizing the total cost rate of the system is considered the thermo-economic objective in the present investigation. A multi-objective variant of the heat transfer search (HTS) algorithm is adopted to perform thermo-economic optimization. The objective function of the thermo-economic optimization problem can be described as follows,

$$Maximize/Minimize\, f(X) = f_1(X), f_2(X) \tag{32}$$

$$X = [x_1, x_2, \ldots\ldots, x_k] \tag{33}$$

where $f_1(X)$ and $f_2(X)$ are exergy efficiency (Eq. (18)) and total cost rate (Eq. (19)) of the CRS respectively. X denotes the set of operating variables that decide both objectives' value.

In the present work, four operating variables of the CRS such as evaporator temperature (T_{eva}), condenser temperature (T_{cond}), LTC condensing temperature ($T_{ltc\text{-}cond}$), and cascade condenser temperature difference (dT) are considered for the optimization during the thermo-economic investigation. The upper and lower bounds of the considered operating variables are given in Table 1.

The CRS's energy, exergy, and economic modeling is carried out in MATLAB R2021(a). The open-source software COOLPROP is used to obtain the thermo-physical properties of R41-R1233zd(E) and R170-R1233zd(E). COOLPROP is integrated with MATLAB during the present investigation. Further, the optimization algorithm used in the present work is also coded in MATLAB. The overview of the complete thermo-economic optimization is presented in Fig. 2.

The optimization algorithm used for the thermo-economic investigation is described in the next section.

4. Heat transfer search (HTS) algorithm and its multi-objective variant

Heat transfer search (HTS) is a population-based metaheuristic algorithm inspired by the natural laws of thermodynamics and heat transfer [28]. The HTS algorithm mimics any system's thermal equilibrium behavior while interacting with its surroundings to achieve a stable state. A system attains thermal equilibrium when its temperature level is the same as the surroundings. Any system transfers heat from conduction, convection, and radiation with the surroundings. Likewise, the search mechanism of the HTS algorithm is composed of three phases. Looking at the analogy between the thermal equilibrium behavior of the system and the HTS algorithm, the system is composed of molecules that resemble the population of the HTS algorithm, the temperature level of the molecules resembles the value of design variables, and the energy level of the system resembles the fitness value of the objective function [29,30].

As mentioned earlier, the search mechanism of the HTS algorithm is executed in three phases: conduction, convection, and radiation. Each phase is executed with equal probability during optimization. The probability band of the conduction phase is 0.−0.3333, that of the convection phase is 0.3333–0.6666, and that of the radiation phase is 0.6666–1. Any of the above-mentioned phases are executed during every generation to update the solution. Further, the greedy selection process is also incorporated into the HTS algorithm so that better solutions can proceed for the next generation.

The HTS algorithm is initiated with the random generation of populations (say $j = 1, 2, 3,\ldots,n$). The design variables (say $i = 1, 2, 3,\ldots,m$) assign an initial evaluation of the objective function to the generated population. Then, the solutions are updated through a predefined number of generations (say 'N_g') either by the conduction phase, convection phase, or radiation phase. The search mechanism of the conduction, convection, and radiation phases simulates "Fourier's law of heat conduction", "Newton's law of cooling", and "the Stefan Boltzmann law", respectively, demonstrated mathematically as below.

Table 1
Operating variables and bounds.

Operating variables	Bounds
Evaporator temperature, T_{eva} (°C)	$-50 \le T_{eva} \le -21$
Condenser temperature, T_{cond} (°C)	$37 \le T_{cond} \le 55$
LTC condenser temperature, $T_{ltc\text{-}cond}$ (°C)	$-6 \le T_{ltc-cond} \le 6$
CCTD, (°C)	$2 \le dT \le 8$

4.1. Conduction phase

$$y_{j,i}' = \begin{cases} y_{k,i} + \left(-R^2 y_{k,i}\right), & if\ f(y_j) > f(y_k) \\ y_{j,i} + \left(-R^2 y_{j,i}\right), & if\ f(y_j) < f(y_k) \end{cases} ; if\ N_g \le N_{g,max} \Big/ C_d F \tag{34}$$

$$y_{j,i}' = \begin{cases} y_{k,i} + \left(-r_i y_{k,i}\right), & if\ f(y_j) > f(y_k) \\ y_{j,i} + \left(-r_i y_{j,i}\right), & if\ f(y_j) < f(y_k) \end{cases} ; if\ N_g > N_{g,max} \Big/ C_d F \tag{35}$$

where, $y'_{j,i}$ is the updated solution; C_dF is the convection factor; the probability of the conduction phase is decided randomly between 0 and 0.3333 and represented by R; the uniformly distributed random number between 0 and 1 is represented by r_i; $N_{g,\max}$ represents the maximum number of generation respectively.

4.2. Convection phase

$$y_{j,i}' = y_{j,i} + R(y_s - T_c F * y_{ms}) \tag{36}$$

$$TCF = \begin{cases} abs(R - r_i), & if\ N_g \le N_{g,max}/C_o F \\ round(1 + r_i) + \left(-R^2 y_{j,i}\right), & if\ N_g > N_{g,max}/C_o F \end{cases} \tag{37}$$

where C_oF is the convection factor; the probability of the convection phase is between 0.6666–1 and represented by R; r_i is the uniformly distributed number between 0 and 1. y_s represent the surrounding temperature (best solution) while y_{ms} is the mean temperature (average solution) of the system; T_cF represents the temperature change factor.

4.3. Radiation phase

$$y_{j,i}' = \begin{cases} y_{j,i} + R\left(y_{k,i} - y_{j,i}\right), & if\ f(y_j) > f(y_k) \\ y_{j,i} + R\left(y_{j,i} - y_{k,i}\right), & if\ f(y_j) < f(y_k) \end{cases} ; if\ N_g \le N_{g,max} \Big/ R_d F \tag{38}$$

$$y_{j,i}' = \begin{cases} y_{j,i} + r_i\left(y_{k,i} - y_{j,i}\right), & if\ f(y_j) > f(y_k) \\ y_{j,i} + r_i\left(y_{j,i} - y_{k,i}\right), & if\ f(y_j) < f(y_k) \end{cases} ; if\ N_g > N_{g,max} \Big/ R_d F \tag{39}$$

where R_dF is the radiation factor; the probability of radiation phase is between 0.3333 - 0.6666 and represented by R.

A non-dominated sorting heat transfer search (NSHTS) algorithm is a multi-objective variant of the HTS algorithm capable of handling multiple objectives simultaneously. The proposed NSHTS algorithm used a non-dominated sorting approach to sort the populations into the different non-dominated levels. Further, the NSHTS algorithm used a crowding distance approach to create and maintain the diversity in the solutions obtained. The updated solutions are stored in the external archives and presented as Pareto points and Pareto front. More details related to the multi-objective variant can be obtained from references [31–33].

5. Case study, result discussion, and comparative analysis

In this work, a two-stage CRS (as shown in Fig. 1) is analyzed with R1233zd(E) HTC refrigerant for the possible substitution of R161 HTC refrigerant. R1233zd(E) is investigated with R41 and R170 LTC refrigerants. The thermophysical properties of each of these refrigerants are provided in Table 2. A two-stage CRS having 50 kW capacity is investigated for its thermo-economic performance. The required cooling temperature for the system considered is 252 K – 223 K, depending upon the application. Both LTC and HTC systems are considered as superheated cycles. The operating specification of the considered system for evaluating its thermal performance is defined in Table 3. Likewise, the parameters required to evaluate the capital and maintenance cost, operating cost, and environmental cost are also provided in Table 3. The HTS algorithm is implemented to obtain the optimization results. The control parameters of the HTS algorithm are given in Table 4. The results

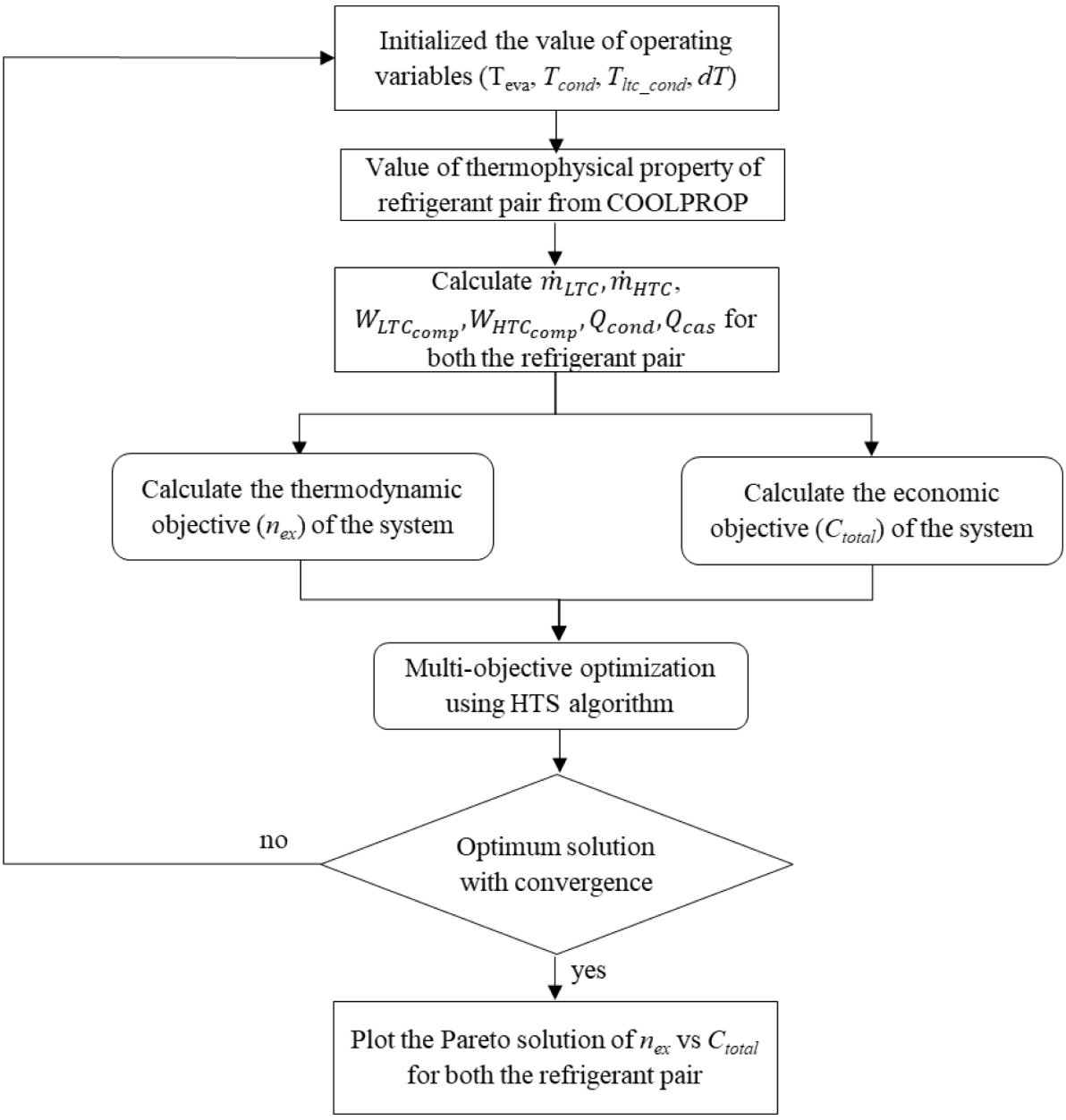

Fig. 2. Framework of optimization.

Table 2
Thermo-physical properties of refrigerants [36].

Refrigerant	$T_{boiling}$ (°C)	$T_{critical}$ (°C)	$P_{critical}$ (bar)	ODP	GWP	ASHRAE safety code
R41	−78.31	44.13	58.97	0	107	A2
R170	−88.58	32.3	48.72	0	20	A3
R1233zd (E)	18.26	166.5	36.24	0	7	A1
R161	−37.5	102	51	0	12	A3

are obtained for both R41-R1233zd(E) and R170-R1233zd(E) based systems and compared with the R41-R161 and R170-R161for the possible substitution of R161. Further, the detailed comparison between R41-R1233zd(E) and R170-R1233zd(E) system is also provided for the possible selection of the refrigerant combination.

The comparative results of both R41-R1233zd(E) and R170-R1233zd (E) based CRS are presented in Fig. 3 in the form of Pareto solutions. It can be observed from the results that the maximum exergy efficiency of R41-R1233zd(E) and R170-R1233zd(E) based CRS are 65.8% and 64.93% with a total plant cost rate of 75,573 $.year^{-1} and 75,121 $.year^{-1}, respectively. Likewise, the minimum cost rates of the two systems are 57,064 $ year^{-1} (R41-R1233zd(E)) and 57,582 $.year^{-1} (R170-R1233zd(E)) with corresponding exergy efficiencies of 63.31% and 62.53%, respectively. For better insight, the optimization results of the five sample design points and the value of the operating parameters are provided in Table 5. The results show a 3.93% variation in exergy efficiency with a 32.43% variation in total cost rate between both extreme solutions of R41-R1233zd(E) CRS. Likewise, for R170-R1233zd(E) CRS, the corresponding variation is 3.83% (exergy efficiency) and 30.45% (total cost rate) respectively. Further, for the same total cost rate of the system (75,121 $.year^{-1}), the R41-R1233zd(E) based CRS gives a higher exergy efficiency (65.75%) as compared to the R170-R1233zd(E) based system (64.93%). In the same way, for the same exergy efficiency, the total plant cost of the R41-R1233zd(E) based CRS is less when compared with the R170-R1233zd(E) based system.

Table 3
Operating specification and economic parameters of CRS [15].

Parameter	Value
Cooling load, Q_{eva}	50 kW
Isentropic efficiency of LTC & HTC compressor, η_s	80%
Dead state temperature, T_0	25 °C
Superheating in LTC & HTC	5 °C
Overall heat transfer coefficient of evaporator, U_{eva}	0.03 kW.m^{-2}.K^{-1}
Overall heat transfer coefficient of condenser, U_{cond}	0.04 kW.m^{-2}.K^{-1}
Cascade condenser overall heat transfer coefficient, U_{cas}	1 kW.m^{-2}.K^{-1}
Temperature difference of air in evaporator and condenser	10 °C
Temperature of the inlet air to the evaporator	−10 °C
Maintenance factor, ϕ	1.06
Interest rate, i	14%
Plant life time, n	15 years
Annual operational hours, N	4266 h
Electrical power cost, α_{elec}	0.09 $\$.kWh^{-1}$
Emission factor, μ_{CO_2e}	0.968 $kg.kWh^{-1}$
Cost of CO_2 avoided, C_{CO_2}	0.09 $\$.kg^{-1}$ of CO_2 emission

Table 4
Control parameters of the HTS algorithm.

Population size: 50
Function evaluation: 10,000
C_dF : 2
C_oF : 10
R_dF : 2

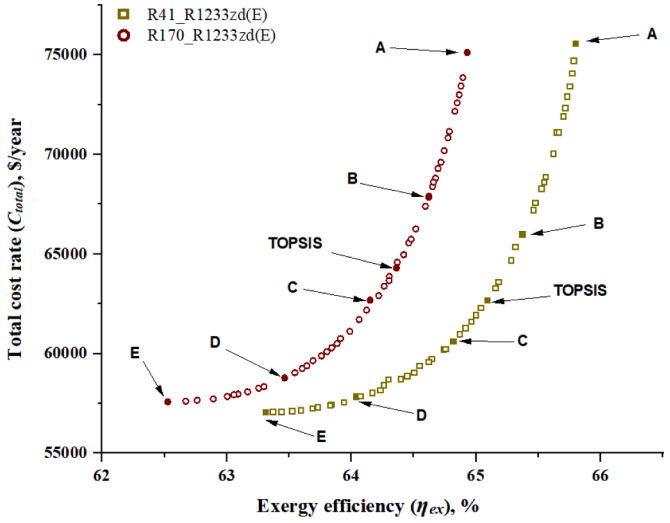

Fig. 3. Pareto optimal solution of R41-R1233zd(E) and R170-R1233zd(E) based CRS.

Fig. 4 shows the comparative results of R41-R161 and R170-R161 based CRS with R41-R1233zd(E) and R170-R1233zd(E) based systems. The R41-R161 and R170-R161 based CRS were investigated by Roy and Mandal [8] and the results are reproduced in the present work for the comparative analysis. It can be observed from the results that the maximum exergy efficiencies of the R41-R161 and R170-R161based CRS are 64.04% and 63.08%, respectively, which are less when compared with R41-R1233zd(E) and R170-R1233zd(E) based systems. Further, for the same total cost rate of the CRS (68,612 $\$.year^{-1}$), the exergy efficiencies of the systems are 63.08% (R170-R161), 64.02% (R41-R161), 64.86% (R170-R1233zd(E)), and 65.55% (R41-R1233zd (E)). For any value of exergy efficiency more than 63.5%, R41-R1233zd (E) and R170-R1233zd(E) based CRS operated with less total cost rate when compared with R41-R161 & R170-R161 based systems. Hence, the comparative results support the possible substitution of HTC refrigerant R161 with R1233zd(E) in CRS.

The Pareto curve offers multiple optimal solutions satisfying the objective functions [34]. The decision-making method TOPSIS [35] is adopted to select the best results from the Pareto solution of Fig. 3. The detailed methodology of TOPSIS is provided by [36]. The result selected by TOPSIS is shown in Fig. 3 and listed in Table 6. The result selected by TOPSIS is further used for the detailed performance comparison between R41-R1233zd(E) and R170-R1233zd(E) based CRS.

Fig. 5 shows the operating variables' effect on CRS's exergy efficiency. It can be observed from the results that the exergy efficiency of both CRS increases with the rise in evaporator temperature. Likewise, the exergy efficiency of both CRS is reduced with increases in condenser temperature, LTC condensing temperature, and cascade condenser temperature difference (CCTD). However, the effect of CCTD is profound on the exergy efficiency followed by the condenser and LTC condensing temperatures. This behavior of exergy efficiency is due to the change in compressor work with the change in operating variables. Further, it can be observed from Fig. 5(a) – (d) that for any value of operating temperature, R41-R1233zd(E) gives higher exergy efficiency as compared to

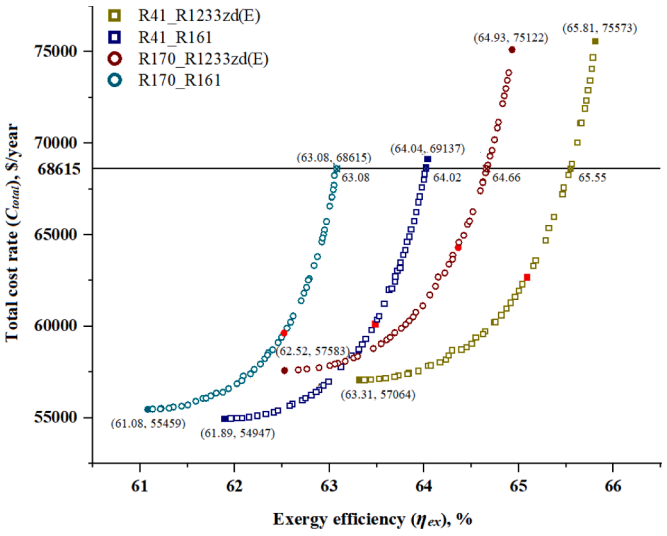

Fig. 4. Comparative results of HTC refrigerant R1233zd(E) and R161 (with R41 and R170 LTC refrigerant) based CRS.

Table 5
Optimized operating variables with thermo-economic objectives of sample design point (A-E) of CRS for both refrigerant pair.

	R41-R1233zd(E)					R170-R1233zd(E)				
	A	B	C	D	E	A	B	C	D	E
Evaporator temperature, (°C)	252.15	249.63	246.98	242.63	240.76	252.15	250.4	247.14	245.17	241.17
Condenser temperature (°C)	310.15	312.26	315.23	318.08	321.95	310.15	311.74	312.97	317.68	322.11
LTC condensing temperature (°C)	271.06	270.41	270.04	269.38	267.15	267.61	267.24	267.19	267.15	267.15
CCTD (°C)	2	2	2	2	2	2	2	2	2	2
Exergy efficiency (%)	65.8	65.37	64.819	64.04	63.31	64.93	64.62	64.15	63.46	62.53
Total plant cost ($.year^{-1})	75,573	65,990	60,606	57,832	57,064	75,121	67,851	62,694	58,781	57,582

Table 6
Optimum result selected by TOPSIS method for CRS with both the refrigerant pairs.

	R41-R1233zd(E)	R170-R1233zd(E)
Evaporator temperature (°C)	248.64	249.35
Condenser temperature (°C)	314.33	313.24
LTC condensing temperature (°C)	270.98	267.19
CCTD (°C)	2	2
Exergy efficiency (%)	65.09	64.36
Total plant cost ($.year^{-1})	62,681	64,297

R170- R1233zd(E).

Fig. 6 presents the effect of operating variables on the cost rates of each component of R41-R1233zd(E) and R170-R1233zd(E) based CRS. A noticeable rise in the evaporator cost rate is observed with the rise in evaporator temperature (Fig. 6(a) and (b)). Further, the cost rates of LTC & HTC compressor and condenser are reduced while the cascade condenser's cost rate remains almost the same with the evaporator temperature rise. With the rise in evaporator temperature, heat transfer between the cooling space and the evaporator is reduced (due to a reduction in LMTD between the evaporator and cooling space). Hence, a larger size evaporator is required to achieve the desired cooling load (50 kW in the present case), which in turn increases the cost of the evaporator. Likewise, with the rise in evaporator temperature, compressor work is reduced (due to a reduction in pressure ratio), which reduces the cost of the compressor and condenser.

The cost rate of a condenser is reduced while the HTC compressor increases with the rise in condenser temperature (Fig. 6(c) and (d)). At a higher condenser temperature, the size of the condenser is reduced due to a higher LMTD (hence less heat transfer area is required) which in turn reduces the cost of a condenser. However, a rise in pressure ratio (p_6/p_5) at a higher condenser temperature increases the cost rate of the HTC compressor. The cost rates of the evaporator, LTC compressor, and cascade condenser are less or more invariable with respect to condenser temperature.

Fig. 6(e) and (f) show the effect of LTC condensing temperature on the cost rate of different components. With the rise in LTC condensing temperature, the cost rate of the LTC compressor increases (due to increases in the pressure ratio p_2/p_1) while that of the HTC compressor is reduced (due to reduction in the pressure ratio p_6/p_5). Further, the condenser cost rate increases while the marginal reduction in evaporator cost is observed with the rise in LTC condensing temperature. Fig. 6(g) and (h) show the effect of CCTD. A marginal rise in the cost rate of the cascade condenser is observed with the increases in CCTD. Further, the cost rate of the HTC compressor also increases (due to a rise in the pressure ratio p_6/p_5) at higher CCTD. The cost rates of evaporator, condenser, and LTC compressor are almost invariable with respect to CCTD.

Fig. 7(a) – (d) shows the effect of operating variables on the total plant cost rate of the R41-R1233zd(E) and R170-R1233zd(E) based CRS. It can be observed from Fig. 7(a) that the total cost rate of the CRS is reduced with an increase in evaporator temperature and reaches a minimum value (due to the dominance of reduction in LTC and HTC compressor work and condenser size over a rise in evaporator size). Then afterwards, a rapid rise in total cost rate is observed with increases in evaporator temperature (due to the dominance of rise in evaporator cost compared to reduction in the cost of other components). Similarly, it can be seen from Fig. 7(b) that the total cost rate is reduced with increases in condenser temperature up to a certain level (due to dominance in reduction of condenser cost over other components) followed by the marginal increment afterwards. The change in the total cost rate of both the CRS is almost identical with respect to variation in

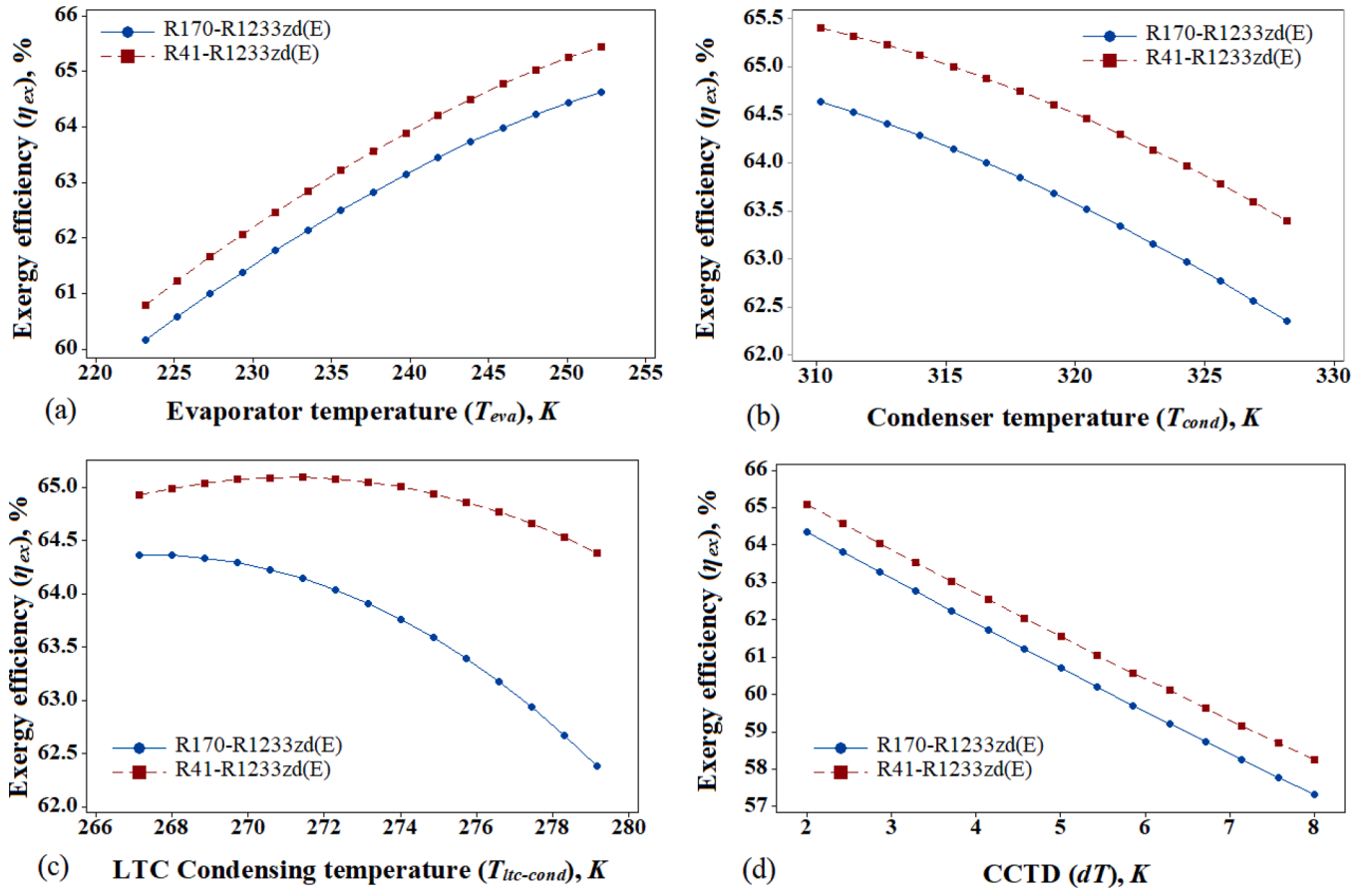

Fig. 5. Effect of operating variables on exergy efficiency of the CRS (a) T_{eva}, (b) T_{cond}, (c) $T_{ltc\text{-}cond}$, (d) dT.

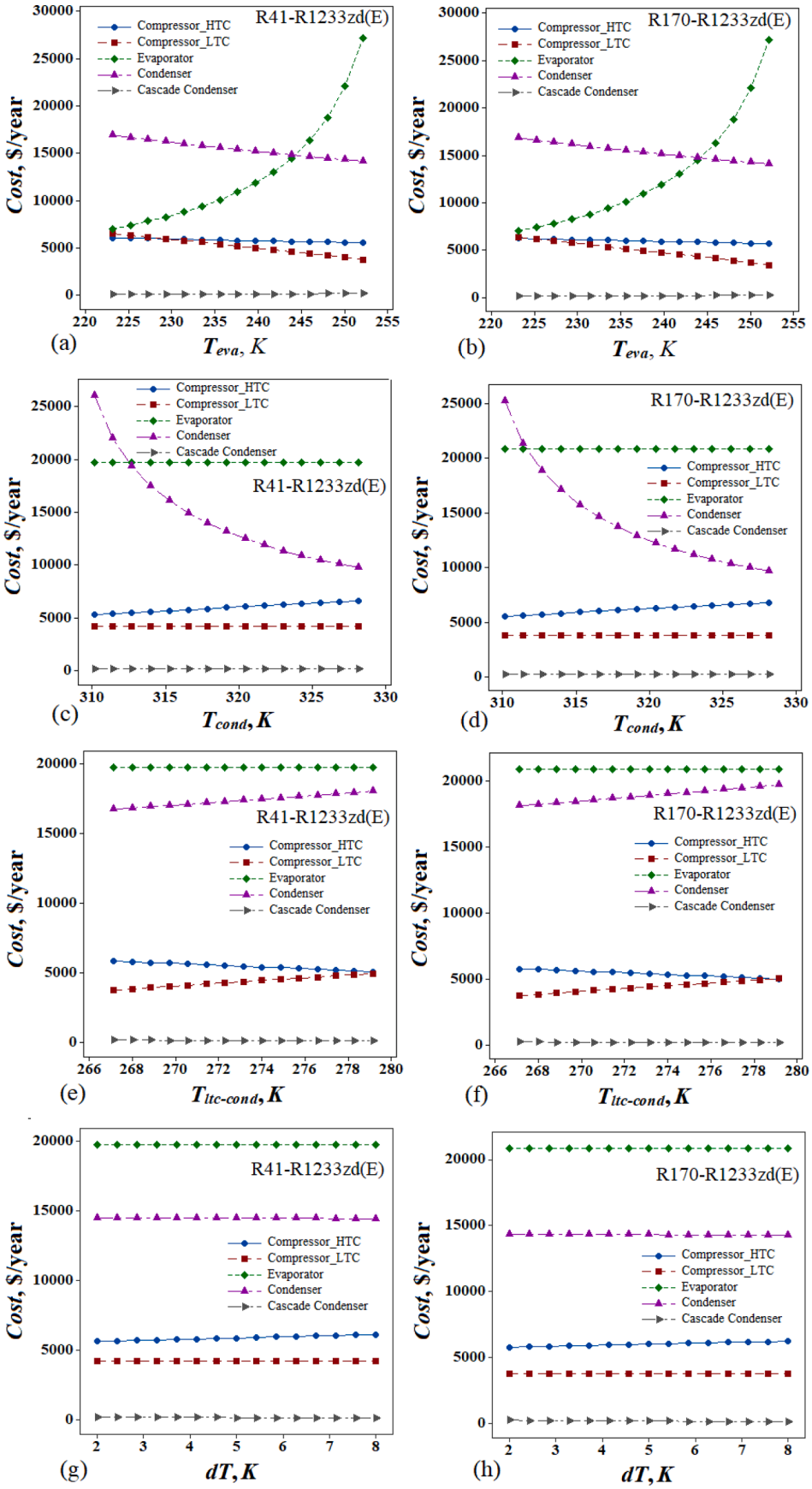

Fig. 6. Effect of operating variables on the component cost rate of CRS (a) & (b) T_{eva}, (c) & (d) T_{cond}, (e) & (f) $T_{ltc\text{-}cond}$, (g) & (h) dT.

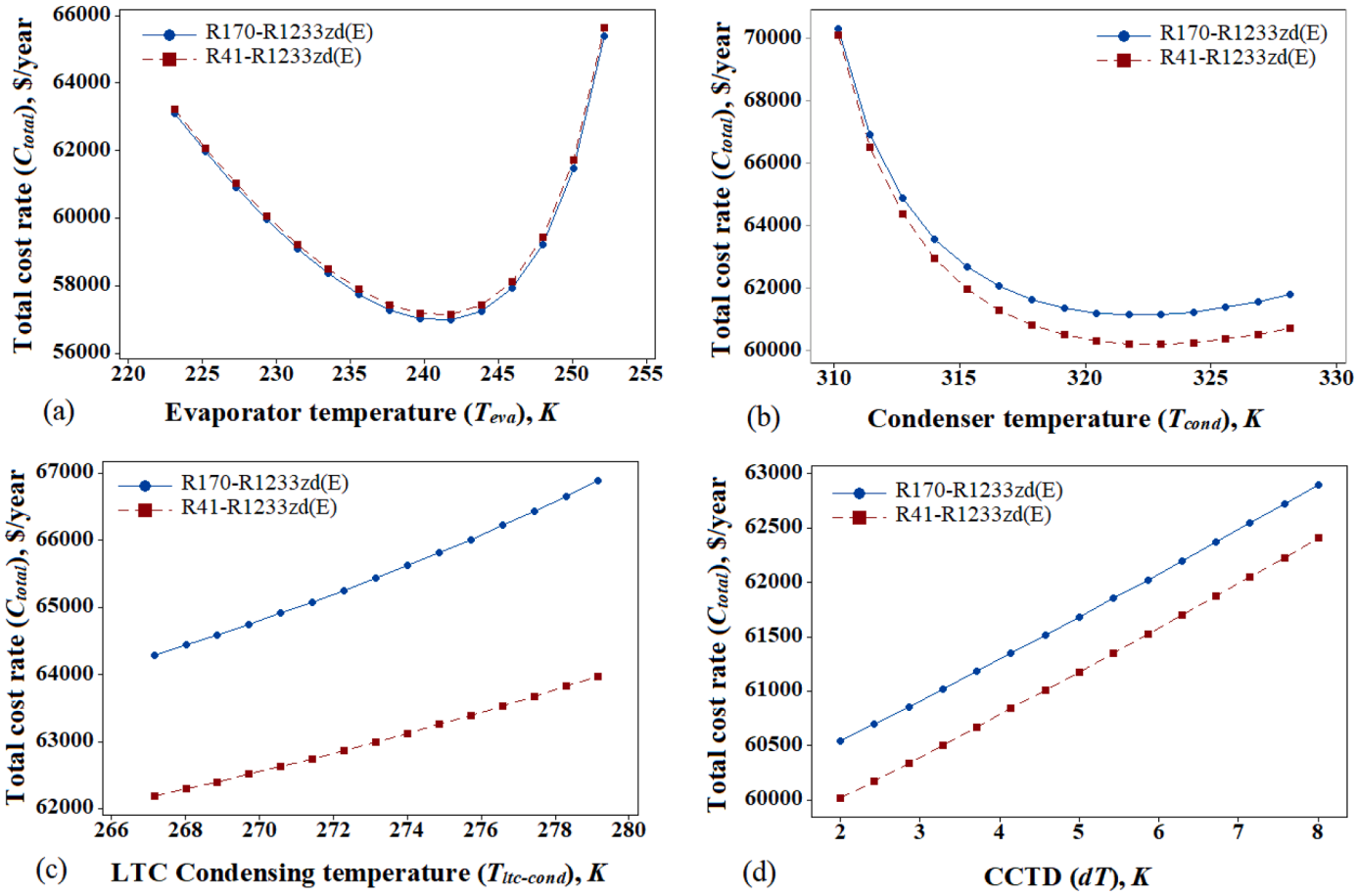

Fig. 7. Effect of operating variables on total cost rate of the CRS (a) T_{eva}, (b) T_{cond}, (c) $T_{ltc\text{-}cond}$, (e) dT.

evaporator temperature. However, the variation in the total cost rate of R41-R1233zd(E) based CRS is higher compared to the R170-R1233zd(E) based system concerning condenser temperature. The total cost rate of both the CRS increases with a rise in LTC condensing temperature (Fig. 7 (c)) and CCTD (Fig. 7(d)). However, the total cost rate difference between the CRS is higher for LTC condenser temperature than CCTD.

The effect of operating variables on the Pareto optimal solutions of R41-R1233zd(E) and R170-R1233zd(E) based CRS is also investigated to identify the sensitivity of operating variables on thermo-economic objectives. For the said investigation, sample design points A – E of Fig. 3 (for both the refrigerant combinations) are considered. Fig. 8(a)–(h) shows the effect of operating variables on the thermo-economic objectives of both the CRS. The increases in exergy efficiency with the corresponding reductions in total cost rates are observed for both the CRS with a rise in evaporator temperature (Fig. 8(a) and (b)). After reaching a minimum cost, further rises in evaporator temperature (T_{eva}) result in simultaneous increases in both objectives. The effect of T_{eva} is more profound on the total cost rate as compared to exergy efficiency. Likewise, the simultaneous reduction in both exergy efficiency and total cost rate is observed with increases in condenser temperature (T_{cond}) for both refrigerant combinations (Fig. 8(c) and (d)). However, a marginal rise in the total cost rate is observed towards the latter part of the condenser temperature. The effect of T_{cond} is almost equal on the thermo-economic objective of both the CRS. Fig. 8(e) and (f) show the effect of LTC condensing temperature (T_{ltc_cond}) on the optimized value of objectives for both refrigerant combinations. It can be observed from the figure that the effect of T_{ltc_cond} is more significant on the total cost rate as compared to exergy efficiency. The effect of CCTD on optimized results for both the CRS is shown in Fig. 8(g) and (h). A linear reduction in exergy efficiency with a corresponding rise in total cost rate is observed with the rise in CCTD (dT) for both refrigerant combinations. The effect of dT is observed more on exergy efficiency than the total cost for both CRS.

Finally, the distribution of operating variables corresponding to the Pareto solution of Fig. 3 for both the CRS is presented in Fig. 9(a)–(d). It can be observed from the figure that the distribution of $T_{ltc\text{-}cond}$ (Fig. 9 (c)) is almost invariable for the R170-R1233zd(E) based CRS while marginal variation in distribution is observed for R41-R1233zd(E). Likewise, the distribution of dT (Fig. 9(d)) is also invariable for CRS with both refrigerant combinations. The scattered distribution of T_{eva} (Fig. 9(a)) and T_{cond} (Fig. 9(b)) is observed for both refrigerant combinations over the entire operating range.

6. Conclusion

In the present work, an attempt is made to investigate the possible substitution of refrigerant R161 (A2 ASHRAE code) by R1233zd(E) (A1 ASHRAE code) for the high-temperature circuit of a CRS. Two-stage R41-R1233zd(E) and R170-R1233zd(E) based CRS are investigated from the thermo-economic viewpoint and compared with R41-R161 and R170-R161 based CRS. The system's efficiency and total cost rate (composed of capital and maintenance, operating, and environment cost) are considered as evaluation criteria to assess the thermo-economic performance of the CRS. The results show that for the same cost rate of the system (68,615 $/year^{-1}), R41-R1233zd(E) based CRS gives 2.39% higher exergy efficiency compared to R41-R161 based CRS. Also, R41-R1233zd(E) and R170-R1233zd(E) based CRS operated with less total cost rate as compared to R41-R161 and R170-R161 based systems.

Further, the TOPSIS decision-making method is adopted to select the best result from the Pareto solutions of both refrigerant combinations.

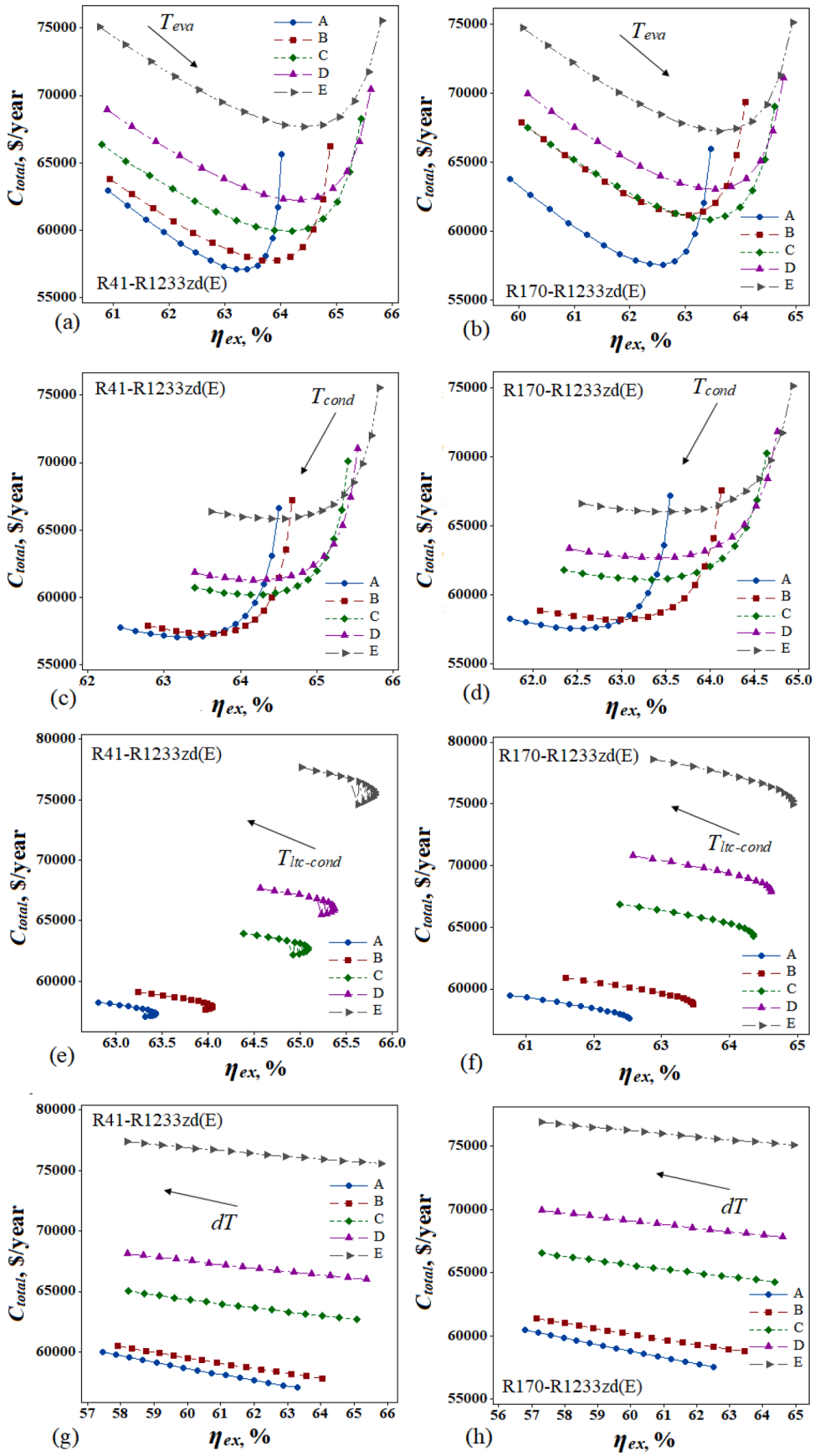

Fig. 8. Sensitivity of operating variables on Pareto solution (A-E) of CRS with both refrigerant combinations.

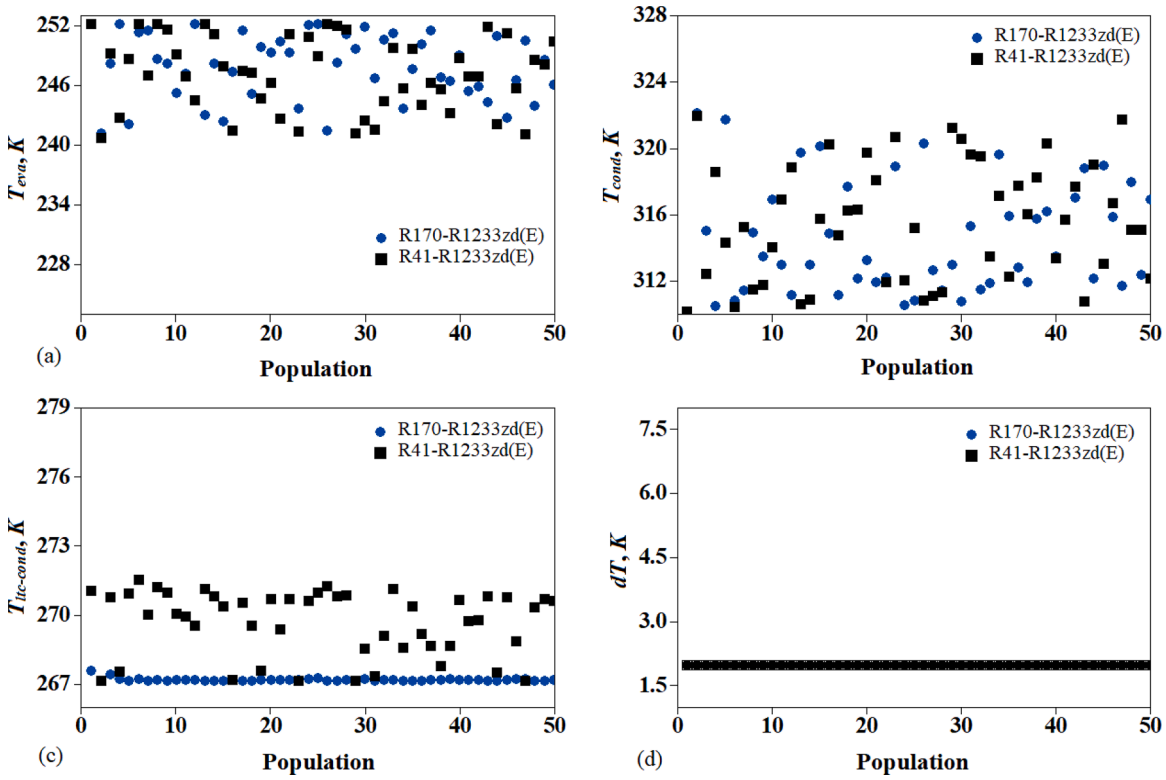

Fig. 9. Distribution of operating variables corresponding to Pareto solution of CRS with both refrigerant combinations.

The effects of operating variables on the thermo-economic objective of R41-R1233zd(E) and R170-R1233zd(E) based CRS are evaluated. The results indicate that all four operating variables create a conflict between thermo-economic objectives. The operating variables' sensitivity to the optimized value of objectives is also evaluated. Evaporator temperature and CCTD appear to be more sensitive to thermo-economic objectives as compared to other operating variables. Finally, based on the comparative results, R41-R1233zd(E) based CRS seems to be an excellent alternative to R41-R161 based CRS.

Declaration of Competing Interest

The authors declare that they have no known competing financial interests or personal relationships that could have appeared to influence the work reported in this paper.

Data availability

Data will be made available on request.

Acknowledgements

The work is done as part of the collaboration between Pandit Deendayal Energy University and the Heat Pipe and Thermal Management Research Group at Brunel University London, UK.

References

[1] P. Prajapati, V. Patel, H. Jouhara, An efficient optimization of an irreversible Ericsson refrigeration cycle based on thermo-ecological criteria, Therm. Sci. Eng. Prog. (2022), 101381, https://doi.org/10.1016/J.TSEP.2022.101381 pJun.

[2] N. Çobanoğlu, A. Banisharif, P. Estellé, Z.H. K.aradeniz, The developing flow characteristics of water - ethylene glycol mixture based Fe3O4 nanofluids in eccentric annular ducts in low temperature applications, Int. J. Thermofluids 14 (2022), 100149, https://doi.org/10.1016/J.IJFT.2022.100149 volpMay.

[3] H. Jouhara, T. Nannou, H. Ghazal, R. Kayyali, S.A. T.assou, S. Lester, Temperature and energy performance of open refrigerated display cabinets using heat pipe shelves, Energy Procedia 123 (2017) 273–280, https://doi.org/10.1016/J.EGYPRO.2017.07.240, volpp.

[4] M.W. F.aruque, M.R. U.ddin, S. Salehin, M.M. E.hsan, A comprehensive thermodynamic assessment of cascade refrigeration system utilizing low GWP hydrocarbon refrigerants, Int. J. Thermofluids 15 (2022), 100177, https://doi.org/10.1016/J.IJFT.2022.100177 volpAug.

[5] R. Lizarte, M.E. P.alacios-Lorenzo, J.D. M.arcos, Parametric study of a novel organic Rankine cycle combined with a cascade refrigeration cycle (ORC-CRS) using natural refrigerants, Appl. Therm. Eng. 127 (2017) 378–389, https://doi.org/10.1016/J.APPLTHERMALENG.2017.08.063, volppDec.

[6] M. Pan, H. Zhao, D. Liang, Y. Zhu, Y. Liang, G. Bao, A review of the cascade refrigeration system, Energies 2020 13 (9) (2020) 2254, https://doi.org/10.3390/EN13092254. Vol. 13, Page 2254volnopMay.

[7] J. Liu, Y. Liu, J. Yu, G. Yan, Thermodynamic analysis of a novel ejector-enhanced auto-cascade refrigeration cycle, Appl. Therm. Eng. 200 (2022), https://doi.org/10.1016/J.APPLTHERMALENG.2021.117636 volJan.

[8] M.O. M.cLinden, A.F. K.azakov, J.Steven Brown, P.A. D.omanski, A thermodynamic analysis of refrigerants: possibilities and tradeoffs for Low-GWP refrigerants, Int. J. Refrig. 38 (1) (2014) 80–92, https://doi.org/10.1016/J.IJREFRIG.2013.09.032, volnoppFeb.

[9] V. Adebayo, M. Abid, M. Adedeji, M. Dagbasi, O. Bamisile, Comparative thermodynamic performance analysis of a cascade refrigeration system with new refrigerants paired with CO2, Appl. Therm. Eng. 184 (2021), https://doi.org/10.1016/J.APPLTHERMALENG.2020.116286 volFeb.

[10] P.A. D.omanski, R. Brignoli, J.S. B.rown, A.F. K.azakov, M.O. M.cLinden, Low-GWP refrigerants for medium and high-pressure applications, Int. J. Refrig. 84 (2017) 198–209, https://doi.org/10.1016/J.IJREFRIG.2017.08.019, volppDec.

[11] C. Aktemur, I.T. O.zturk, C. Cimsit, Comparative energy and exergy analysis of a subcritical cascade refrigeration system using low global warming potential refrigerants, Appl. Therm. Eng. 184 (2021), 116254, https://doi.org/10.1016/J.APPLTHERMALENG.2020.116254 volpFeb.

[12] Z. Sun, Q. Wang, Z. Xie, S. Liu, D. Su, Q. Cui, Energy and exergy analysis of low GWP refrigerants in cascade refrigeration system, Energy 170 (2019) 1170–1180, https://doi.org/10.1016/J.ENERGY.2018.12.055, volppMar.

[13] A. Ustaoglu, B. Kursuncu, M. Alptekin, M.S. G.ok, Performance optimization and parametric evaluation of the cascade vapor compression refrigeration cycle using Taguchi and ANOVA methods, Appl. Therm. Eng. 180 (2020), 115816, https://doi.org/10.1016/J.APPLTHERMALENG.2020.115816 volpNov.

[14] Z. Sun, Q. Wang, B. Dai, M. Wang, Z. Xie, Options of low global warming potential refrigerant group for a three-stage cascade refrigeration system, Int. J. Refrig. 100 (2019) 471–483, https://doi.org/10.1016/J.IJREFRIG.2018.12.019, volppApr.

[15] R Roy, B.K Mandal, Thermo-economic analysis and multi-objective optimization of vapour cascade refrigeration system using different refrigerant combinations,

J. Therm. Anal. Calorim. 139 (5) (2019) 3247–3261, https://doi.org/10.1007/S10973-019-08710-X, 2019 1395volnoppAug.
[16] F. Yilmaz and R. Selbaş, 'Comparative thermodynamic performance analysis of a cascade system for cooling and heating applications', vol. 16, no. 9, pp. 674–686, Jul. 2019, doi: 10.1080/15435075.2019.1618308.
[17] K.Kumar Singh, R. Kumar, A. Gupta, Comparative energy, exergy and economic analysis of a cascade refrigeration system incorporated with flash tank (HTC) and a flash intercooler with indirect subcooler (LTC) using natural refrigerant couples, Sustain. Energy Technol. Assessments 39 (2020), 100716, https://doi.org/10.1016/J.SETA.2020.100716 volpJun.
[18] V. Patel, D. Panchal, A. Prajapati, A. Mudgal, P. Davies, An efficient optimization and comparative analysis of cascade refrigeration system using NH3/CO2 and C3H8/CO2 refrigerant pairs, Int. J. Refrig. 102 (2019) 62–76, https://doi.org/10.1016/J.IJREFRIG.2019.03.001, volppJun.
[19] M.M. K.eshtkar, P. Talebizadeh, Multi-objective optimization of a R744/R134A cascade refrigeration system: exergetic, economic, environmental, and sensitive analysis (3ES), J. Therm. Eng. 5 (4) (2019) 237–250, volnopp.
[20] Y Ust, A.S Karakurt, Analysis of a cascade refrigeration system (CRS) by using different refrigerant couples based on the exergetic performance coefficient (EPC) criterion, Arab. J. Sci. Eng. 39 (11) (2014) 8147–8156, https://doi.org/10.1007/S13369-014-1335-9, 2014 3911volnoppSep.
[21] A.H. Mosaffa, L.G. Farshi, C.A. Infante Ferreira, M.A. R.osen, Exergoeconomic and environmental analyses of CO2/NH3 cascade refrigeration systems equipped with different types of flash tank intercoolers, Energy Convers. Manag. 117 (2016) 442–453, https://doi.org/10.1016/J.ENCONMAN.2016.03.053, volppJun.
[22] Y. Qin, N. Li, H. Zhang, B. Liu, Energy and exergy performance evaluation of a three-stage auto-cascade refrigeration system using low-GWP alternative refrigerants, Int. J. Refrig. 126 (2021) 66–75, https://doi.org/10.1016/J.IJREFRIG.2021.01.028, volppJun.
[23] F. Yilmaz, R. Selbaş, Energy and exergy analyses of CO2/HFE7000 cascade cooling system, Süleyman Demirel Univ. J. Nat. Appl. Sci. 21 (3) (2017) 854–860, https://doi.org/10.19113/SDUFBED.58140, volnoppOct.
[24] ASHRAE, ANSI/ASHRAE standard 34-2019', Des. Saf. Classif. Refrig. Am. Soc. Heating, Refrig. Air-Conditioning Eng. (2019).
[25] I. Dincer, M.A. Rosen, P. Ahmadi, Optimization of energy systems, Optim. Energy Syst. (2017) 1–453, https://doi.org/10.1002/9781118894484, ppJan.
[26] M. Aminyavari, B. Najafi, A. Shirazi, F. Rinaldi, Exergetic, economic and environmental (3E) analyses, and multi-objective optimization of a CO2/NH3 cascade refrigeration system, Appl. Therm. Eng. 65 (1–2) (2014) 42–50, https://doi.org/10.1016/J.APPLTHERMALENG.2013.12.075, volnoppApr.
[27] J. Wang, Z.J. Z.hai, Y. Jing, C. Zhang, Particle swarm optimization for redundant building cooling heating and power system, Appl. Energy 87 (12) (2010) 3668–3679, https://doi.org/10.1016/J.APENERGY.2010.06.021, volnoppDec.
[28] V.K. P.atel, V.J. S.avsani, Heat transfer search (HTS): a novel optimization algorithm, Inf. Sci. (Ny). 324 (2015) 217–246, https://doi.org/10.1016/J.INS.2015.06.044, volppDec.
[29] P.P. Prajapati, V.K. Patel, Thermo-economic optimization of a nanofluid based organic Rankine cycle: a multi-objective study and analysis, Therm. Sci. Eng. Prog. 17 (2020), https://doi.org/10.1016/j.tsep.2019.100381 vol.
[30] P.P. Prajapati, V.K. Patel, Comparative analysis of nanofluid-based organic Rankine cycle through thermoeconomic optimization, Heat Transf. - Asian Res. 48 (7) (2019) 3013–3038, https://doi.org/10.1002/htj.21528, volnopp.
[31] B.D. Raja, R.L. Jhala, V. Patel, Thermal-hydraulic optimization of plate heat exchanger: a multi-objective approach, Int. J. Therm. Sci. 124 (2018) 522–535, https://doi.org/10.1016/J.IJTHERMALSCI.2017.10.035, volppFeb.
[32] B.D. Raja, R.L. Jhala, V. Patel, Many-objective optimization of cross-flow plate-fin heat exchanger, Int. J. Therm. Sci. 118 (2017) 320–339, https://doi.org/10.1016/J.IJTHERMALSCI.2017.05.005, volppAug.
[33] V.K. Patel, An efficient optimization and comparative analysis of ammonia and methanol heat pipe for satellite application, Energy Convers. Manag. 165 (2018) 382–395, https://doi.org/10.1016/J.ENCONMAN.2018.03.076, volppJun.
[34] Y.A.A. Laouid, C. Kezrane, Y. Lasbet, A. Pesyridis, Towards improvement of waste heat recovery systems: a multi-objective optimization of different organic Rankine cycle configurations, Int. J. Thermofluids 11 (2021), 100100, https://doi.org/10.1016/J.IJFT.2021.100100 volpAug.
[35] H. Aljaghoub, F. Abumadi, M.N. A.lMallahi, K. Obaideen, A.H. Alami, Solar PV cleaning techniques contribute to sustainable development goals (SDGs) using Multi-criteria decision-making (MCDM): assessment and review, Int. J. Thermofluids 16 (2022), 100233, https://doi.org/10.1016/J.IJFT.2022.100233 volpNov.
[36] C.-L. Hwang, K. Yoon, Multiple Attribute Decision Making, 1st ed., 186, Springer Berlin Heidelberg, Berlin, Heidelberg, 1981 vol.